FINITE ELEMENT MODELING OF THE PRINCE OF WALES FORT WALL FAILURE

A. Isfeld[1], N. Shrive[2]
[1] PhD Candidate, Department of Civil Engineering, University of Calgary Schulich School of Engineering, Calgary, AB, T2N 1N4, Canada, acisfeld@ucalgary.ca
[2] D.Phil., Professor, Department of Civil Engineering, University of Calgary Schulich School of Engineering, Calgary, AB, T2N 1N4, Canada, ngshrive@ucalgary.ca

ABSTRACT
The Prince of Wales Fort was constructed in the 18th century in the Vauban style, with ashlar face stones encasing a core of rubble stone masonry. The fort is located in Churchill Manitoba, and has thus been subjected to extreme weather conditions. The exposure has caused severe degradation and washout of the original mortar creating highly variable core conditions, which have led to lateral deformation of sections of the wall in some areas, and collapse in others. Restoration of the severely damaged sections was begun within the last decade, but meanwhile, sections of wall that were previously in good condition have begun to show signs of distress. Development of a conservation plan to prevent degradation of the undamaged wall sections was deemed essential.

A two dimensional finite element model has been formulated to represent the in-situ conditions of a damaged wall section. The model was created in Abaqus and focuses on the case of self weight. Micro-modelling techniques were employed to model the stones individually and define the behaviour of interactions between the individual stones. The resulting displacements have been examined, and compared to the actual displacements as well as the results of discrete element modeling. Beginning with a model of a deteriorated wall section will provide a basis upon which a variety of restoration methods can later be investigated.

KEYWORDS: finite element modeling, discrete element modeling, masonry, restoration, structural analysis

INTRODUCTION
The Hudson Bay Trading Company (HBC) constructed the Prince of Wales Fort (shown in Figure 1a) at the mouth of the Churchill River, across the river from present day Churchill, Manitoba. The fort was constructed to safeguard the local trading post against the French, with whom the English were competing for trade dominance. Construction began in 1731 and was completed over 40 years by a small team of men [1]. After 10 years of occupation and trading, an attack by the French caused the fort to be abandoned, remaining unoccupied for 150 years. In the 1920's the fort was recognized as being of national significance by the Historic Sites and Monuments Board of Canada and was acquired by the Parks Branch of the Department of the Interior (currently Parks Canada). The rationale for this significant recognition is due both to the fort's status as the most northerly construction of its kind, and to it being a physical commemoration of the historic French-English rivalry over the bay and its resources. Parks

Canada took responsibility for the conservation of the fort, and through the 1930's work was done to remedy the damage that had occurred during its time left abandoned.

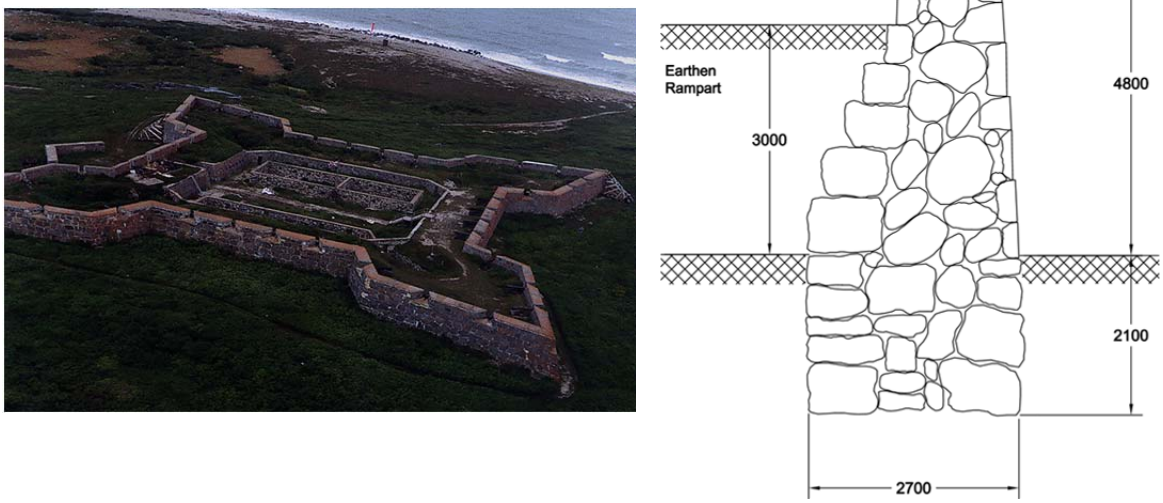

(a) (b)

Figure 1: (a) Prince of Wales Fort aerial view (photo courtesy of the Canadian Military History Gateway) (b) Wall cross section with dimensions in mm

The escarp wall of the fort is comprised of a rubble masonry core with ashlar face stones on the exterior and above the surface of the rampart on the interior. The total height of the wall sections, including a 1.8 m parapet, is 4.8 m and the foundation continues 2.1 m underground and is 2.7 m wide. Behind the wall lies an earthen and gravel backfill which reaches a height of 3 m. A general schematic, cross-sectional view is provided in Figure 1b.

Two local stone types were used to construct the fort; Churchill quartzite and dolostone with compressive strengths of 186 MPa and 188 MPa respectively [2]. During the first ten years of construction, split boulder face stones and mud (or clay) mortar were used. Lime mortar was used on the outer wythe when the ashlar face stones were placed, during the later portion of the construction. These ashlar face stones are regularly shaped in only one plane. Given the high compressive strength of the stones, it was favourable to cut only the exposed face of the stones, while the backs were left uncut and thus taper off irregularly. The face and side views of two face stones in Figure 2 show the high degree of variance in the size and shape. Similarly, the stones within the core of the wall were left uncut, as they would not be visible. Core stones up to 2 m in diameter have been found. When initially placed, both the lime and clay mortars acted primarily as filler materials due to their low compressive strengths. While these mortars are inherently weak, the cold climate would have hindered the curing process necessary for the lime mortar to gain significant strength [2]. Much of the mortar has been washed out, or severely degraded within the wall leaving a highly irregular assembly with stones bearing on each other,

rather than being bonded by mortar. The exception to this unbonded state is at the top of the parapets where, during the 1930's restoration work, concrete was poured till refusal.

Figure 2: Comparison of two face stones removed from the north wall

In response to visible deformations, a stabilization program was initiated in 2003 by Public Works and Government Services Canada. Several locations were identified for structural stabilization, where there were lateral displacements or partial collapse near the mid height of the wall. The stabilization was achieved through local dismantling and rebuilding or permanent shoring. Over the last decade new sections of the ashlar walls have shown accelerated deformation. Having performed well in the past, these new problems have been cause for alarm, as they indicate insufficient understanding of the structural stability of the walls. In light of this gap in knowledge, it is clear that a better understanding of the stability of the escarp wall and its failure mechanism is essential. This understanding will be developed using both finite and discrete element modeling and will assist in the selection of a methodology for stabilizing the walls.

DISCRETE ELEMENT MODEL

The initial goal was to understand the effect of bonding within the walls on the stability of the wall sections. Discrete Element Modeling (DEM) was performed with the non-smooth contact dynamics method (NSCD) in the LMGC90 program [3-6]. This modelling revealed that a transition from instability to stability could always be made by increasing the bond strength (the reverse of what may have happened over time). Five wall sections were modelled with simplified convex geometric shapes, varying the geometry in both the core material and the outer wythe, with a consistent profile for the back and top of the wall (Figure 3). Repeated runs of the model were executed with different coefficients of friction, increasing the normal component of the cohesion until stability was achieved. Stability was always achieved in these inherently unstable cross sections with some coefficient of friction. The initial deformations during the failures of the models resembled the in-situ deformations of the walls, with lateral bulging near mid height as can be seen in Figure 4.

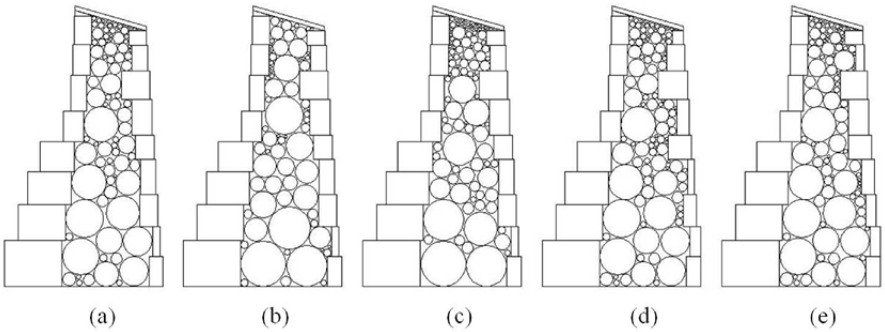

Figure 3: Five cross sections for DEM

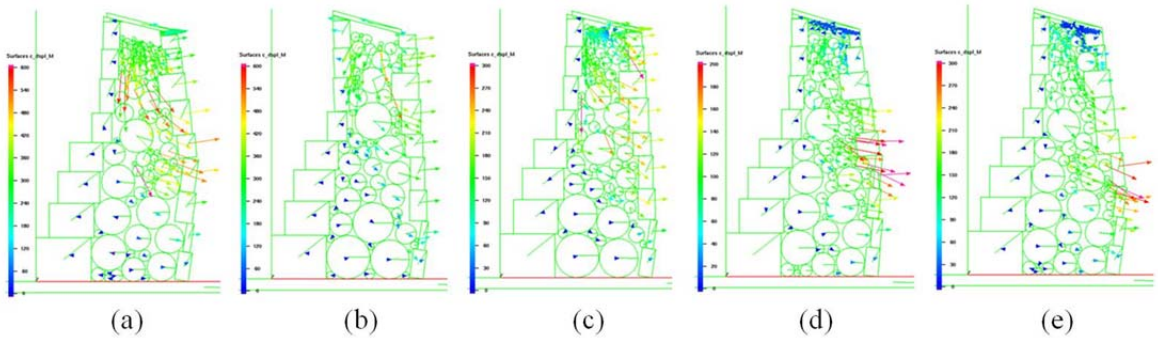

Figure 4: Deformed cross sections from DEM showing displacement vectors

FINITE ELEMENT MODEL INTRODUCTION

Based on the ability of these unstable DEM cross-sections to transition to a state of stability at a given bond strength, the option of increasing the bond strength by means of grout injection needed more detailed assessment. Finite Element Modeling (FEM) was implemented as it would allow for the study of more complex and realistic geometry, as well as the addition of grout within the void space. The issue was how to develop a model that represents the current in-situ deformations.

FEM of masonry structures can be executed on three possible scales, detailed micro-modelling, simplified micro-modeling, and macro-modeling [7]. Macro-modeling is not suitable for this application as it applies to solid structures with known macro properties. Thus detailed or simplified micro-modeling are the most viable options for the current modeling goals. Simplified micro-modeling was used to create a base model onto which varying conditions and restoration measures could be applied. Masonry assemblies can be modeled with continuum elements as a single material, using contact elements to represent the joint behaviour [8]. Using this methodology, the unknown properties of the in-situ mortar will be excluded, and the interactions between the stones in the wall will be modeled instead. With base model established, detailed micro-modeling will be invoked to determine specific material properties required for injected grout. This will be done by modeling the stones and grout separately, with individual material properties and realistic contact interactions as in Ali and Page [9].

GEOMETRY

The geometry of the face stones for the model was taken from stones removed during the ongoing restoration work (some examples were shown in Figure 2), representing a vertical cut in

the north wall. The geometry of the foundation stones and the backing stones are based on those established in a cross section developed at the onset of the restoration program. As limited data are available on the geometry of the stones within the core of the wall, stone shapes were traced from images taken of the core of the wall, and the stones were assembled within the core of the wall to best resemble these images, while fitting within the face and backing stones. The geometry was drafted in AutoCAD 2013, and imported as a sketch to Abaqus where the spline function was used to smooth the edges of the shapes. Each stone within the cross section was input into Abaqus as a separate part with a plane stress strain thickness of 1 m. An initial model (Figure 5a) corresponding to the geometry in Figure 1b was used, as well as two additional models with localized variations shown in Figure 5. The first change (Figure 5b and c) replaced a small round stone with a flat stone to prevent the small stone from rolling and increasing the displacement of the face stone it supports. Next the bearing area of the narrow face stone was increased from 30 mm to 60 mm on the bottom and from 25 mm to 60 mm on the top (Figure 5d). Two mesh densities are shown in Figure 5 that will be discussed further.

MATERIAL PROPERTIES

Only the compressive strength of the stones has been established, so assumed values have been used for the modulus, density and Poisson's ratio of the stones as given in Table 1. In-situ crushing of the stones has not been observed; rather rolling and sliding dominate the wall failure. Subsequently material properties that allow rigid body movements rather than local deformations will most accurately represent the actual conditions.

Table 1: Material Properties

Property	Value
Density, ρ	2000 kg/m^3
Young's Modulus, E	20 GPa
Poisson's Ratio, υ	0.3

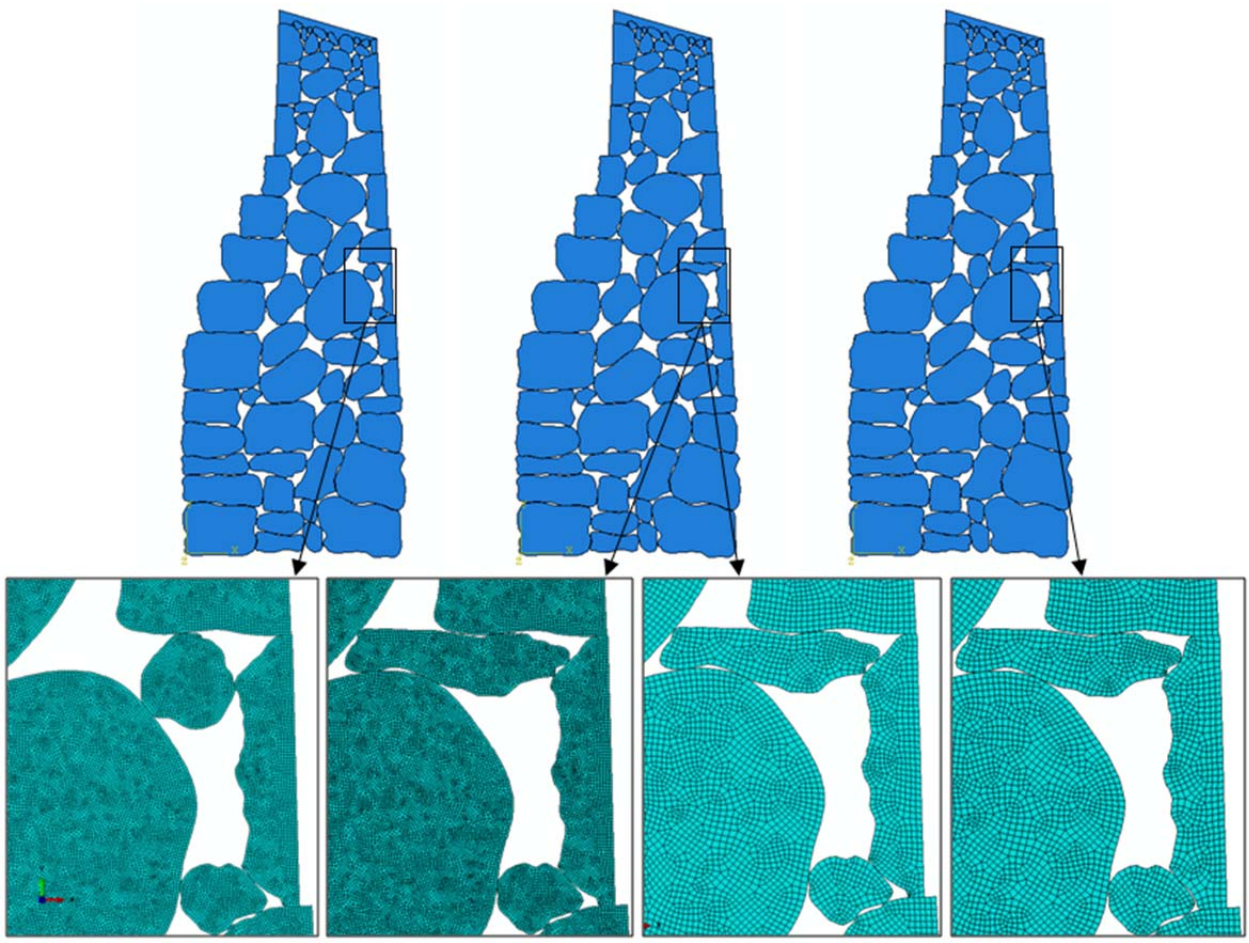

(a) (b) (c) (d)

Figure 5: Three cross sections used for FEM with average element sizes of 0.007 (a and b) and 0.015 (c and d)

BOUNDARY CONDITIONS

The boundary conditions were considered fixed in the vertical direction along the base, and fixed in the horizontal direction up to the ground level on the outer foundation face and to the top of the earthen rampart on the inner face. These simplified boundary conditions have been used as a starting point, active and passive soil pressure will be included as the model progresses.

LOADING

For this preliminary model, only self weight was considered for the load. All stones, as well as the concrete cap were considered to have the same density, as was assumed in the DEM. Self weight is seen as the most critical load, as it is the internal conditions rather than the external loading that is of interest in this model.

CONTACT

In choosing between assigning contact in a general, or a pair-wise manner there is a trade off between ease of contact definition and analysis performance. A pair-wise defined contact will compute more efficiently, but definition of contacts is much simpler when general contact is used [10]. For this model, due to the large number of parts in contact, and the potential for contact pairs to evolve over the simulation, general contact was defined for all surfaces within

the assembly. The general contact method uses a surface-to-surface discretization method and considers the shape of both the master and slave surfaces when the contact constraints are defined. Rather than selecting individual master and slave surfaces for each contact pair, the general contact algorithm enforces an average sense between interacting surfaces and automatically assigns master and slave roles. The magnitude of the relative motion was defined as finite sliding as large displacements were anticipated. Finite sliding is expensive computationally, particularly when multiple deformable bodies are in contact, as it becomes necessary to track which part of the master surface is in contact with each slave node. For surfaces to be in contact they must be separated by a distance that is less than or equal to the separation tolerance, for which default values were used, and the surfaces must be intuitively opposed. This requires that the surfaces be offset from each other by less than 45° at the closest point of approach [10].

Both tangential and normal behaviour were defined for the contact. The normal behaviour was assigned as 'hard contact' using default constraint enforcement with separation allowed after contact. Coulomb friction was used to describe the tangential behaviour and the frictional coefficient μ was set at 0.7. The shear stress limit τ_{crit} is related to the frictional coefficient and the contact pressure between the two surfaces p as

$$\tau_{crit} = \mu p \tag{1}$$

To implement this contact behaviour a penalty friction formulation has been used. This formulation allows for elastic slip, rather than using the ideal stick-slip behaviour and requires less computational power than the Lagrange formulation.

TIME STEPPING

Dynamic implicit step was used over which the load was ramped. Geometric nonlinearity was included in the model so that rotations and deformations of the contact surfaces could be accounted for. A time step of 1 second was modeled to simulate the behaviour immediately after all the mortar was absent from the wall.

MESH REFINEMENT AND ELEMENT FORMULATION

For element based surfaces, faceted geometry dependent on the element mesh, is used. Thus, for a curved surface a coarse mesh may give a poor approximation of the geometry for contact modeling [10]. A high mesh density is required in the model due the presence of many curved surfaces. Multi point constraints (MPC's) could have been used to allow for a fine mesh on the surface of the part instances, with a coarse mesh on the part interior. However the trade-off between the time required to mesh the model with MPC's and the amount of time required to run the simulation led to MPC's being omitted. If master and slave surfaces were to be assigned individually, it would be ideal to mesh the slave surface more finely than the master surface: however since the contact behaviour is enforced in an averaged sense in general contact, a consistent mesh density of continuum elements can be used for the entire model.

Due to the large number of parts in the full model, to simplify the mesh refinement study three small stones (from the top of the wall cross section) were meshed repeatedly to determine a suitable mesh density for the model. The small stones were selected as they interact with the

concrete cap at the top of the model for which the complex geometry will restrict the maximum element size. The average element size (side length) was varied from 0.008 m for the least dense mesh to 0.0015 m for the most dense. Using these varied mesh densities the following element formulations were also studied; linear, linear with incompatible modes, and quadratic. The quadratic formulation was eliminated as a candidate as it produces erroneous stresses in contact due to the method used in the calculation of consistent nodal loads for contact pressure [10]. These erroneous contact stresses are propagated into errors in reaction forces which can be seen in Figure 6a. Linear elements with incompatible modes were also deemed unsuitable for this problem. While incompatible modes can perform well in contact problems, their behaviour degrades quickly when elements move from a square shape to a parallelogram [10], which would be necessary with the complex geometry within the cross section.

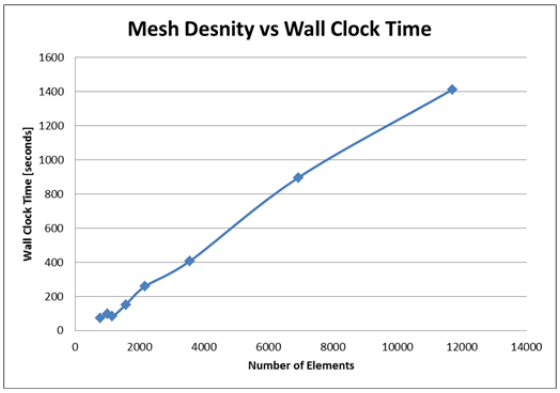

(a) (b)

Figure 6: (a) Reaction forces from contact modeled with quadratic elements. (b) Effect of mesh density on model run time

When linear elements are used the displacements are found to be highly dependent on the mesh density, as can be seen in Figure 7, for which the displacements of the stones are shown compared to the original positions. It is also shown in Figure 6b that a near linear relationship exists between the number of linear elements used and the time taken for the model to run.

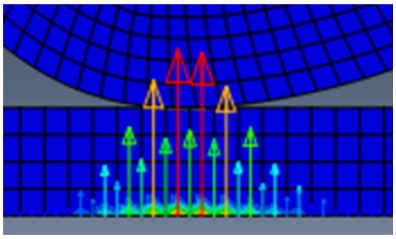

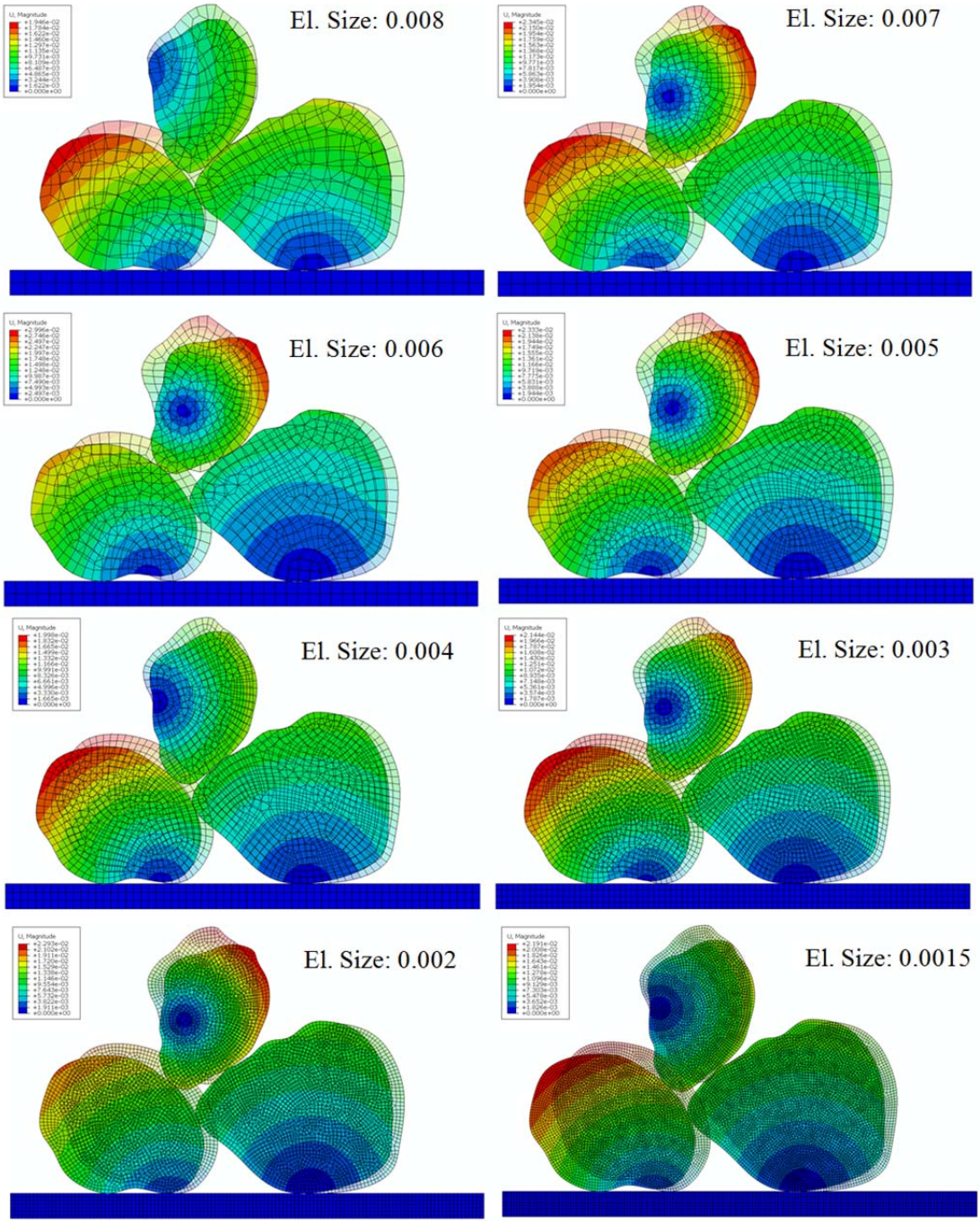

Figure 7: Mesh refinement study on three stacked stones, element size given in meters.

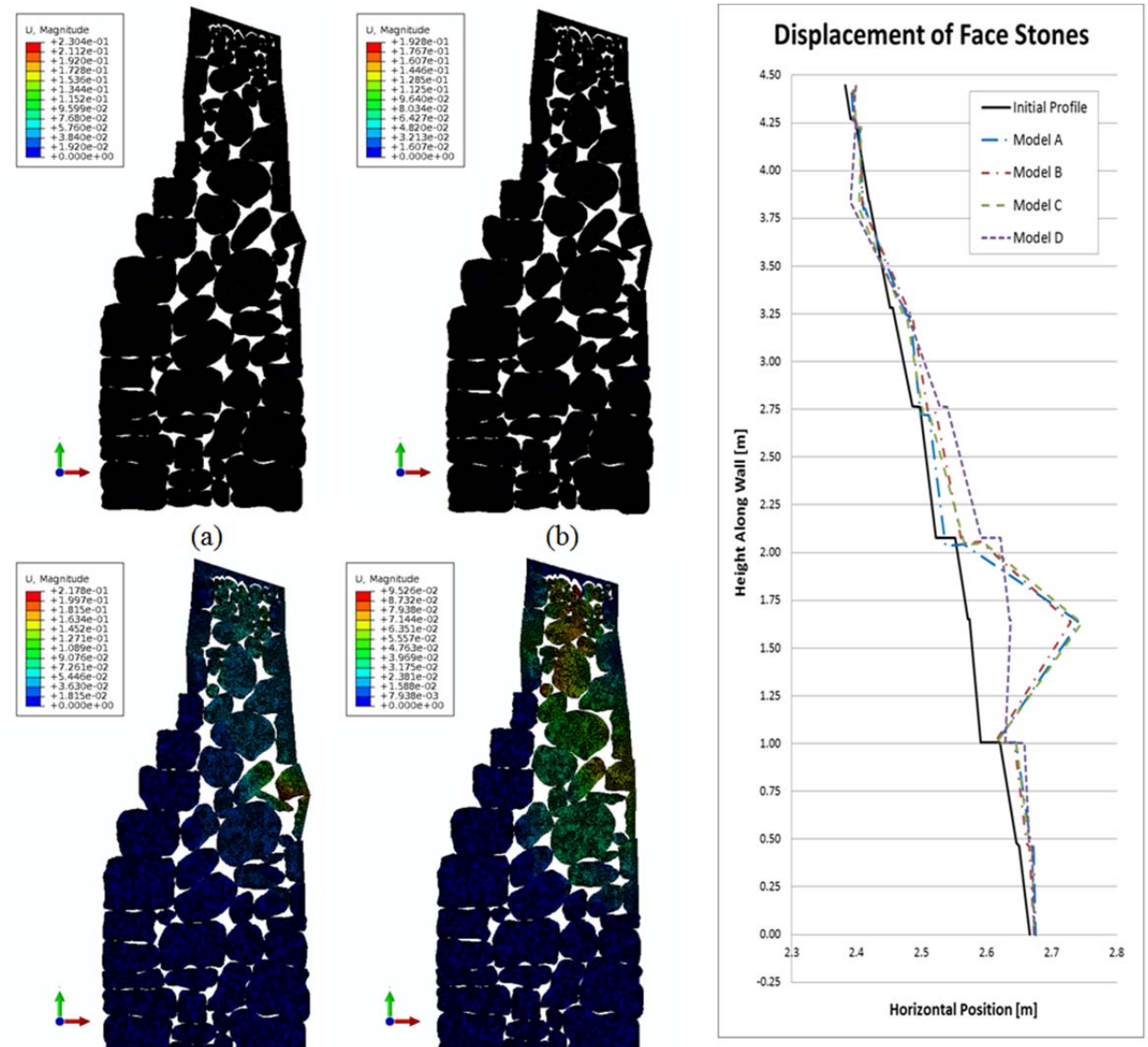

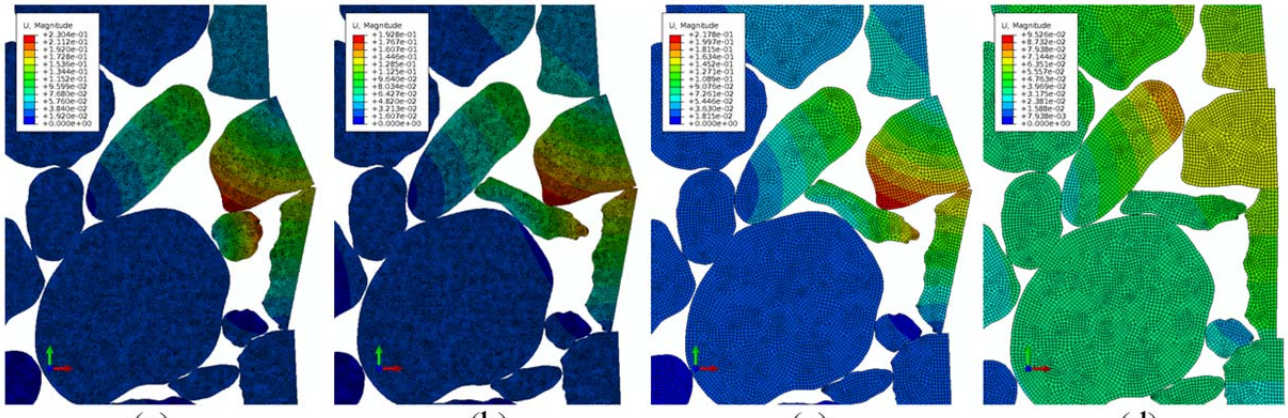

Figure 8: Comparison of displacements of face stones in models A, B, C and D

Based on the data from the mesh refinement exercise, an element size of 0.007 m (Figure 8 a and b) was selected as a starting point. However, a coarser mesh with an average element size of 0.015 m (Figure 8 c and d) was also used to reduce the computation time from 62 to 12 hours. These two meshes, and the models they were applied to, are shown in Figure 5. These four models are referred to as models A through D as given in Table 2.

Table 2: Model Description

Model	Average El. Size [m]	Description
A	0.007	Original geometry
B	0.007	Round core stone replaced with flat stone
C	0.015	Round core stone replaced with flat stone
D	0.015	Bearing area of face stone increased and flat stone in core

RESULTS

The results from the four models can be seen in Figure 8a-d with a comparison of the face stone displacements in Figure 8e. Despite reducing the mesh density significantly, models B and C which have identical geometric properties, gave the same failure mechanism with the maximum displacement increasing from 152 mm to 170 mm with the increased mesh density. Comparing the original geometry of model A with the two variations, it was found that while replacing the round stone with a flat stone did not reduce the horizontal displacements, as expected, increasing the bearing area of the narrow face stone did. Actual values for displacements along the Southeast Bastion are supplied in Figure 9. A summary of the maximum displacements of the four models and the most critical section of the Southeast Bastion is given in Table 3.

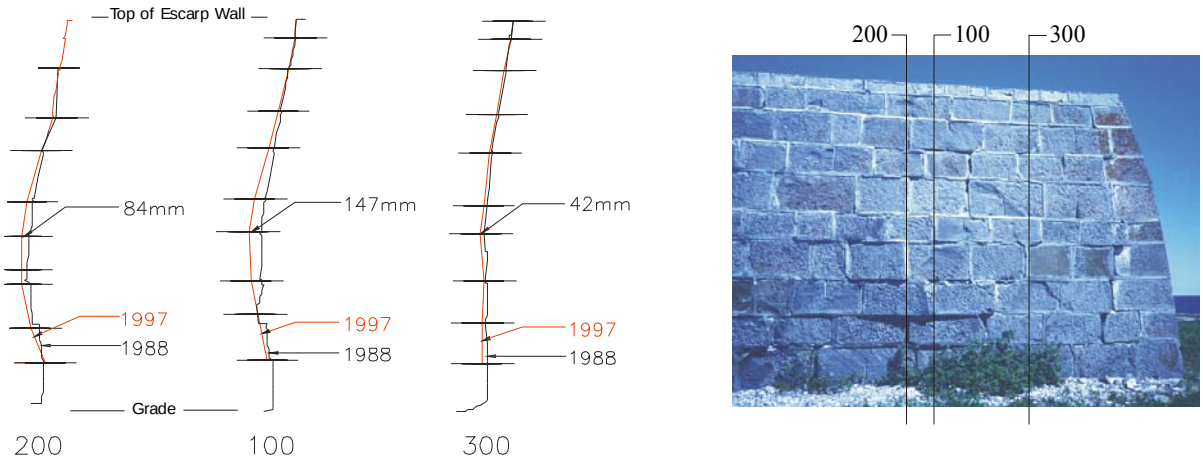

Figure 9: Horizontal displacements on three sections of the Southeast Bastion (HCP, 2000)

Table 3: Values for maximum displacement in four models and Southeast Bastion line 100

	Model A	Model B	Model C	Model D	SE 100
Max Disp. [mm]	164	152	170	64	147

DISCUSSION

It is evident that low bonding between the stones has allowed settling of the core material, causing displacement of the face stones. Comparing Figure 8 and Figure 4 for the FEM and

DEM respectively, it may be observed that while failure of the wall sections does vary depending on both the face stone and core geometry the lateral bulging of the models consistently occurs near the mid-height of the wall. This is also in agreement with the observed deformations and the maximum displacement values for the Southeast Bastion of the fort.

Having developed models that produce similar failure mechanism to those shown by the fort walls, restoration techniques can now be explored using the models. A detailed study of grout injection will be done by adding continuum elements within the voids, then applying a variety of material properties and contact behaviour to this material. Rock anchors could be tested by linking the face stone to stones within the wall. Determining the optimal restoration technique will require studying both the effect of the measures on the wall section, and the practicality of applying these measures on site. Choosing the most suitable restoration option will help maintain the structural integrity of this historically significant structure.

ACKNOWLEDGEMENTS
The authors gratefully acknowledge the financial support of the Natural Sciences and Engineering Research Council of Canada and the University of Calgary. The help of IT services at the University, and Compute Canada is also gratefully recognized.

REFERENCES

1. Fontaine, L. and Elliot, C. (2007) "Impact of Climate Change on Prince of Wales Fort: The Conservation Process and the Adaptation Strategy" PWGS Canada, Editors.
2. Heritage Conservation Program (2000) "Prince of Wales Fort 1999-2000 Structural Condition Assessment and Recommendations" RPS, et al., Editors.
3. Jourdan, F., Alart, P., and Jean, M. (1998) "A Gauss-Seidel Like Algorithm to Solve Frictional Contact Problems" Computer Methods in Applied Mechanics and Engineering, 155(1-2): p. 31-47.
4. Jean, M. (1999) "The Non-Smooth Contact Dynamics Method" Computer Methods in Applied Mechanics and Engineering, 177(3-4): p. 235-257.
5. Moreau, J.J. (1999) "Numerical aspects of the sweeping process" Computer Methods in Applied Mechanics and Engineering, 177(3-4): p. 329-349.
6. Jean, M., Acary, V., and Monerie, Y. (2001) "Non-Smooth Contact Dynamics Approach of Cohesive Materials" Philosophical Transactions of the Royal Society of London Series a-Mathematical Physical and Engineering Sciences, 359(1789): p. 2497-2518.
7. Lourenco, P.B. (2002) "Computations on historic masonry structures" Progress in Structural Engineering and Materials, 4(3): p. 301-319.
8. Page, A.W. (1978) "Finite Element Model for Masonry". ASCE J Struct DIV, 104(8): p. 1267-1285.
9. Ali, S.S. and Page A.W. (1988) "Finite-Element Model for Masonry Subjected to Concentrated Loads" Journal of Structural Engineering-Asce, 114(8): p. 1761-1784.
10. ABAQUS 6.11 (2011) "ABAQUS 6.11 PDF Documentation" Dassault Systemes Simulia Corp., Providence, RI.